Recent changes in shelf hydrography in the Siberian Arctic: Potential for subsea permafrost instability

Igor A. Dmitrenko,[1] Sergey A. Kirillov,[2] L. Bruno Tremblay,[3] Heidemarie Kassens,[1] Oleg A. Anisimov,[4] Sergey A. Lavrov,[4] Sergey O. Razumov,[5] and Mikhail N. Grigoriev[5]

Received 18 April 2011; revised 1 July 2011; accepted 28 July 2011; published 19 October 2011.

[1] Summer hydrographic data (1920–2009) show a dramatic warming of the bottom water layer over the eastern Siberian shelf coastal zone (<10 m depth), since the mid-1980s, by 2.1°C. We attribute this warming to changes in the Arctic atmosphere. The enhanced summer cyclonicity results in warmer air temperatures and a reduction in ice extent, mainly through thermodynamic melting. This leads to a lengthening of the summer open-water season and to more solar heating of the water column. The permafrost modeling indicates, however, that a significant change in the permafrost depth lags behind the imposed changes in surface temperature, and after 25 years of summer seafloor warming (as observed from 1985 to 2009), the upper boundary of permafrost deepens only by ~1 m. Thus, the observed increase in temperature does not lead to a destabilization of methane-bearing subsea permafrost or to an increase in methane emission. The CH_4 supersaturation, recently reported from the eastern Siberian shelf, is believed to be the result of the degradation of subsea permafrost that is due to the long-lasting warming initiated by permafrost submergence about 8000 years ago rather than from those triggered by recent Arctic climate changes. A significant degradation of subsea permafrost is expected to be detectable at the beginning of the next millennium. Until that time, the simulated permafrost table shows a deepening down to ~70 m below the seafloor that is considered to be important for the stability of the subsea permafrost and the permafrost-related gas hydrate stability zone.

Citation: Dmitrenko, I. A., S. A. Kirillov, L. B. Tremblay, H. Kassens, O. A. Anisimov, S. A. Lavrov, S. O. Razumov, and M. N. Grigoriev (2011), Recent changes in shelf hydrography in the Siberian Arctic: Potential for subsea permafrost instability, *J. Geophys. Res.*, *116*, C10027, doi:10.1029/2011JC007218.

1. Introduction

[2] The Arctic Ocean marginal seas are an important component of the Arctic environment and Earth's climate system. The recent decrease of perennial sea ice during the summer season over the Arctic shelves [*Comiso et al.*, 2008; *Kwok et al.*, 2009; *Stroeve et al.*, 2008; *Kwok and Rothrock*, 2009] has imposed severe changes on the Siberian shelf environment. These include the timing of sea-ice freezeup and breakup [*Markus et al.*, 2009], the offshore migration of the seasonal ice zone [*Mahoney et al.*, 2008], and a substantial increase in the extent and duration of the summer ice-free period when the water column is exposed to solar heating and wind-forced mixing. In addition, the total annual discharges from the six largest Eurasian rivers draining into the Arctic show a positive trend [*Peterson et al.*, 2006] and recently reached an all-time record high in 2007 [*Rawlins et al.*, 2009].

[3] The eastern Siberian shelf, consisting of the Laptev and East Siberian seas, represents the shallowest and broadest shelf region of the entire World Ocean, with an average depth of about 20–30 m and extending a distance of 400–800 km from the shoreline (Figure 1 and Table 1). In contrast, the Beaufort and Chukchi shelves are about 50 to 100 m deep and constitute a rather narrow Arctic shelf region. This topographic feature makes the eastern Siberian shelf very sensitive to the offshore northward seasonal migration of the sea-ice cover as well as to changes in atmospheric circulation. Changes in the offshore summertime pack ice extent and open-water duration are the most important factors controlling the trends in upper layer heat content in this region [*Steele et al.*, 2008].

[4] The eastern Siberian shelf is underlain by relic offshore submarine permafrost in an environment that is favorable for the stability of gas hydrates [*Delisle*, 2000; *Romanovskii et al.*, 2004, 2005]. Submarine permafrost and

[1]Leibniz Institute of Marine Sciences, University of Kiel, Kiel, Germany.
[2]Arctic and Antarctic Research Institute, St. Petersburg, Russia.
[3]Department of Atmospheric and Oceanic Sciences, McGill University, Montreal, Quebec, Canada.
[4]Department of Climate Change Research, State Hydrological Institute, St. Petersburg, Russia.
[5]Melnikov Permafrost Institute, Siberian Branch of the Russian Academy of Science, Yakutsk, Russia.

0148-0227/11/2011JC007218

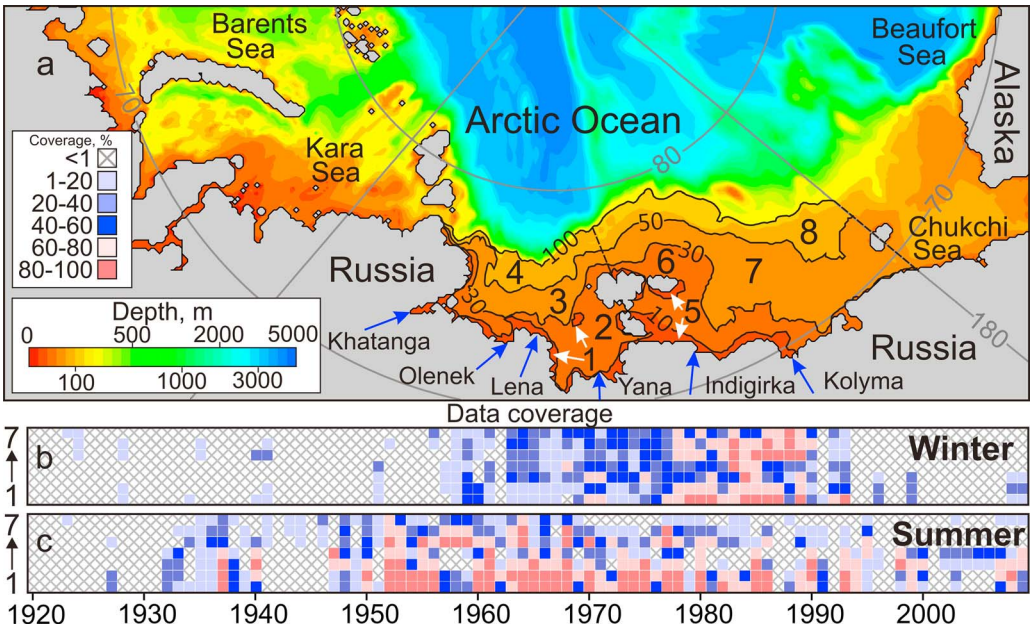

Figure 1. (a) Map of the eastern Arctic Ocean. Solid lines delineate the Laptev (subregions 1–4) and East Siberian (subregions 5–8) sea shelves. Subregions 1 and 5 represent the coastal zone shallower than 10 m. The inner shelf (subregions 2 and 6) and midshelf (subregions 3 and 7) extend from 10 m to 30 m and from 30 m to 50 m in depth, respectively. The outer shelf (subregions 4 and 8) occupies the area between 50 and 100 m depth contours. Rivers with runoff exceeding 20 km^3/summer are shown by the blue arrows. (b, c) The data coverage of the interpolated field (percentage from the entire subregion area) within subregions 1–7 for (b) winter (February–April) and (c) summer (July–September). There is insufficient data for subregion 8. The color code is defined in the legend on the top-left corner of the top panel.

permafrost-related gas hydrate stability zone (GHSZ) are believed to be storing significant amounts of methane [e.g., *O'Connor et al.*, 2010]. The dramatic changes in the Arctic environment in recent years may have wide significance for methane release from the Arctic continental margins if warming of the coastal waters continues and the submarine permafrost becomes thermodynamically unstable. The dissociation of hydrate in response to increased temperature has the potential to produce rapid releases of methane [*Westbrook et al.*, 2009]. Up to now, there has been no evidence that such emissions have yet increased because of global warming [*O'Connor et al.*, 2010]. However, numerous speculations regarding the shelf submarine permafrost degradation and liberation of methane have been proposed recently, with emphasis on a possible implication for further climate changes [*Reagan and Moridis*, 2007; *Westbrook et al.*, 2009; *Shakhova and Semiletov*, 2009; *Shakhova et al.*, 2009, 2010]. Recently, *Shakhova et al.* [2010] reported extensive methane venting in the eastern Siberian shelf and suggested that the subsea permafrost could become unstable in a future warmer Arctic. In response to this statement, *Petrenko et al.* [2010] argued that no persuasive arguments have yet been provided to show that Arctic warming has a role in the observed rate of methane emission.

Table 1. Main Hydrographic Characteristics of the Laptev and East Siberian Sea Subregions Defined in Figure 1

	Laptev Sea				East Siberian Sea			
Subregion	1	2	3	4	5	6	7	8[a]
Depth (m)	<10	10–30	30–50	50–100	<10	10–30	30–50	50–100
Area[b] (10^3 km^2)	17.6	212.4	82.4	69.6	30.4	268.4	244.8	176.8
Summer bottom salinity (psu)	20.68	26.59	32.67	33.83	20.07	26.66	31.82	X
σ (psu)	±1.80	±1.04	±0.60	±0.15	±1.42	±1.02	±0.53	X
Summer bottom temperature (°C)	1.62	−0.13	−1.44	−1.51	1.05	−0.47	−1.37	X
σ (°C)	±1.29	±0.60	±0.19	±0.11	±0.98	±0.41	±0.16	X
Winter bottom salinity (psu)	26.61	28.68	33.04	33.90	23.29	27.67	31.71	X
σ (psu)	±0.92	±0.90	±0.34	±0.23	±1.58	±0.93	±0.41	X
Winter bottom temperature (°C)	−1.43	−1.44	−1.64	−1.61	−1.28	−1.49	−1.66	X
σ (°C)	±0.05	±0.10	±0.06	±0.09	±0.10	±0.07	±0.12	X

[a]Crosses indicate insufficient data.
[b]Area calculations based on the International Bathymetric Chart of the Arctic Ocean (IBCAO, http://www.ngdc.noaa.gov/mgg/bathymetry/arctic/arctic.html).

[5] In this paper we examine the eastern Siberian shelf bottom layer hydrography and in particular the bottom water layer thermal stability with the potential implication for the stability of the submarine permafrost and the permafrost-related GHSZ. This research is directly motivated by recent reports by *Shakhova and Semiletov* [2009] and *Shakhova et al.* [2009, 2010] on the high concentration of methane measured over the eastern Siberian shelf, which, as they suggest, is likely associated with thawing of the underwater permafrost. To this end, we revisit the Russian historical hydrographic data set for the period 1920–2009 in order to examine the modern trend of the bottom layer hydrography associated with climatic changes. We show unequivocal evidence of the bottom layer warming from the middle of 1980s. We also undertake a broader review of the processes that control the seabed warming and discuss the stability of subsea permafrost based on simulation of its sensitivity to the changing shelf environment.

2. Materials and Methods

2.1. Hydrographic, Sea-Ice, and Meteorological Data

[6] The first data set used in this study is the Arctic and Antarctic Research Institute (AARI) hydrographic data set, which consists of summer (July–September) and winter (February–April) salinity and temperature observations (1920–1992) updated with recent summer and winter measurements from 1993 to 2009. Throughout this paper we use the common definition for the summer season ranging from June to September and for the winter season ranging from November to April. This is done despite the fact that there are no hydrographic data available for June and November–January. Winter historical hydrographic data were obtained during Soviet aircraft surveys in the 1960s through the 1990s and more recently from the Russian-German TRANSDRIFT expeditions in 1996, 1999, 2008, and 2009. Summer ship-based observations were collected in the ice-free regions of the Laptev and East Siberian seas in 1920–2008. Over the last several years, this data set has been extensively used to assess the different patterns of the eastern Siberian shelf hydrography (for example, see *Dmitrenko et al.* [2008, 2009]; *Polyakov et al.* [2008]).

[7] From the bottom topography, we subdivide the eastern Siberian shelf into eight subregions (Figure 1). The coastal zone shallower than 10 m represents subregions 1 and 5. The inner shelf (subregions 2 and 6) and midshelf (subregions 3 and 7) extend from 10 m to 30 m and from 30 m to 50 m in depth, respectively. The outer shelf (subregions 4 and 8) occupies an area with depths between 50 and 100 m. The geographical and hydrographical characteristics of these eight subregions are shown in Table 1. The 1920–2009 time series of annual summer (July–September) mean bottom layer temperature (BLT) and bottom layer salinity (BLS) for the Laptev and East Siberian seas subregions (as defined in Figure 1) are calculated by integrating vertically and spatially the annual summer temperature and salinity data over the 5 m thick bottom layer and surface area over each subregion. The data coverage for each subregion is defined in the following manner. All data are first binned into a regular grid with 20 km horizontal resolution, and then the percentage of coverage is defined as the percentage of grid cells in a subregion with data.

[8] To examine the BLS and BLT errors that are due to the scarcity in data coverage of the coastal zone and inner shelf, we calculate the summer mean BLTs and BLSs of 1000 random subdomains covering 0% to 100% of the data-covered subregion area for years when the station data cover is at least 80% of the entire subregion (see Figure 1c). The BLTs and BLSs of the 1000 randomly selected subdomains were calculated and then compared with the true annual BLTs and BLSs calculated from the BLTs and BLSs for the subregion areas covered with data coverage larger than 80%. From the variance in BLTs and BLSs (calculated from the difference between the "true" and the subsampled values) we derive an estimate of the 95% confidence level for the entire subregion. This is shown using error bars in Figures 3c, 3d, 4c, and 4d. This procedure is explained in more detail by *Dmitrenko et al.* [2008].

[9] We use summer (June–September) mean sea-ice extent data over the Laptev and East Siberian seas from the National Snow and Ice Data Center (http://nsidc.org/data/g02182.html) [*Mahoney*, 2008]. These sea-ice time series are derived from the sea-ice charts of the AARI, St. Petersburg (see *Mahoney* [2008] for more details). Monthly mean river discharge data were taken from the Arctic-RIMS (Regional Integrated Monitoring System) data set (http://rims.unh.edu). From this data set, only data from rivers with runoff exceeding 20 km^3 for the whole hydrological summer (defined as the months between river ice break up and freezeup, June–September) were taken into account. Bottom topography was derived from the International Bathymetric Chart of the Arctic Ocean (IBCAO; http://www.ngdc.noaa.gov/mgg/bathymetry/arctic/arctic.html).

[10] The time series of summer (June–September) mean surface air temperature (SAT) and atmospheric pressure (SLP) were calculated from the National Centers for Environmental Prediction (NCEP;1948–2009 time period) data [*Kalnay et al.*, 1996] by averaging over the Laptev and East Siberian seas regions. The summer (June–September) mean SLP data are used to calculate the vorticity of the atmosphere over the adjoining Arctic Ocean. The horizontal resolution of the NCEP-derived data is 2.5° of latitude.

[11] We use a vorticity index to formalize the patterns of atmospheric circulation over the eastern Siberian shelf and adjoining Arctic Ocean. The vorticity index gives both the sign and magnitude of atmospheric vorticity [*Walsh et al.*, 1996]. It is defined as the numerator of the finite difference Laplacian of the SLP for an area within a radius of 550 km centered at 85°N and 125°E, a region located in the Arctic Ocean close to the northeastern Laptev Sea. A negative vorticity index corresponds to an anticyclonic atmospheric circulation, and a positive index corresponds to a cyclonic circulation. Summer (June–September) mean vorticity indices were derived from monthly SLP NCEP data.

2.2. Permafrost Model

[12] We investigate the subsea permafrost response to the summer (July–September) bottom layer warming and freshening observed over the Laptev Sea coastal zone. To this end we use a permafrost model that explicitly takes into account the effect of salt diffusion in the seafloor sediments and the temporal evolution of the temperature and salinity profiles, calculated taking into account the BLT and BLS

seasonal cycling based on our long-term (1920–1984) mean data for the Laptev Sea coastal zone.

[13] The core of the permafrost dynamical model used in this study is based on *Delisle* [2000]. In this model, however, we also include salt diffusion in the bottom sediments following *Anisimov et al.* [2005]. The model accounts for the latent heat at the phase change boundary through adjustment of the volumetric heat capacity when the sediment temperature approaches 0°C. Thermal conductivity depends on the liquid pore water and ice fraction in the sediments. Thermal and mass fluxes are coupled in the model. Following *Anisimov et al.* [2005], the key model equations can be written as

$$c_a \frac{\partial T}{\partial t} = \frac{\partial}{\partial z}\left(\lambda \frac{\partial T}{\partial z}\right) + \rho_w L \frac{\partial W}{\partial t}\vartheta - \rho_w L \frac{\partial W_u}{\partial S}\frac{\partial S}{\partial t}\vartheta, \quad (1)$$

$$\frac{\partial (W_u S)}{\partial t} = \frac{\partial}{\partial z}\left(D_s \frac{\partial S}{\partial z}\right), \quad (2)$$

$$c_a = c + \rho_w L \frac{\partial W_u(T)}{\partial T}\vartheta, \quad (3)$$

where

$$\vartheta = \begin{cases} 0; \ if \ T \geq 0 \\ 0; \ if \ T < 0 \ and \ W \leq W_u(T) \\ 1; \ if \ T < 0 \ and \ W > W_u(T) \end{cases}.$$

[14] In these equations t is the time; dz is the thickness of the element; T is the sediment temperature (°C); L is the latent heat (J/kg); W is the liquid pore water fraction in the sediments, m^3/m^3; ρ_w is the pore water density, kg/m^3; W_u is the unfrozen water content (m^3/m^3), defined as the difference between the liquid pore water fraction and the ice fraction in the pore space; λ is the thermal conductivity of sediments (W/mK); c_a is the effective heat capacity of sediments (J/kg K); c is the specific heat capacity of sediments (J/kg K); S is the salinity of water in the sediment pore space (in practical salinity units, psu); and D_S is the salt diffusion coefficient for the seafloor sediments defined as

$$D_S = D_{S0} W_u / \tau, \quad (4)$$

where D_{S0} is the salt diffusion coefficient for the seawater and τ is the tortuosity factor for the pore space (~1.5). The buoyancy- and density-driven flow processes are not constrained.

[15] The coupling of thermal and mass fluxes is prescribed by the last term in equation (1). Mathematical realization follows that by *Nicolsky and Shakhova* [2010]. Physical constants in the heat diffusion equation are specified following *Anisimov et al.* [2005] and *Nicolsky and Shakhova* [2010]. The geothermal heat flux at the low boundary of frozen sediments was set to 0.06 W/m^2 [*Anisimov et al.*, 2005; *Nicolsky and Shakhova*, 2010].

[16] The model was run with the monthly time step and a vertical resolution of 10 cm. The forcing BLT and BLS data are given by a step function as follows. In the summer (June–September) and winter (November–April) seasons, we set the seafloor temperature and salinity to a constant seasonal-mean BLT and BLS. In the transition season (May and October), we fix the bottom layer temperature and salinity to their mean values between summer and winter.

[17] The initial temperature profile (8000 years B.P.) across the upper 800 m layer of sediments represents a linear temperature distribution from −13.5°C at the surface to 7°C at 800 m, which follows *Delisle* [2000]. During that time, the frozen ground is assumed to be uncontaminated by salt. Approximately 8000 years B.P., the terrestrial permafrost, which presently extends over the east Siberian coastal zone, started to be inundated, and the temperature at its upper boundary was increased by ~12°C, from −13.5°C to −1.5°C [*Fleming et al.*, 1998]. The initial vertical temperature profile for 1985 is set from the output of a paleosimulation starting 8000 years B.P. (before the shelf inundation) until 1985. A long-term (1920–1984) summer-mean BLT = 1.1°C and BLS = 20.9 psu and winter-mean BLT = −1.4 and BLS = 26.6 psu are used to force the model from 8000 years B.P. to 1984. From 1985 to 2100, we impose a linear trend in summer BLTs of 0.09°C/yr, equal to the modern warming trend observed from 1985 to 2009 (see section 3.1 for more details). Afterward, we keep the BLT constant (11.5°C) until the year 3000.

3. Results

3.1. Recent Changes in Siberian Shelf Environment

[18] During the summer (June–September), the eastern Siberian shelf bottom layer hydrography is forced by direct solar radiation heating and heat input from Siberian River runoff. This heat is used in part to warm up the water column and in part to melt sea ice. These result in substantial bottom layer warming over the coastal zone and inner shelf up to 2.0 ± 1.5°C (Figure 2a), and freshening relative to winter ranging from 1 to 5 psu (not shown; for more details see *Dmitrenko et al.* [2010]). During winter, thermodynamic ice formation causes convection that ventilates bottom waters, resulting in cooling (Figure 2b) and salinification of the bottom layer through brine release. This generates a strong seasonal modulation of the thermohaline signal at the base of the water column, particularly in the coastal zone and inner shelf region (Figure 2). In the midshelf and outer-shelf Laptev Sea areas deeper than 30–50 m, we observe a positive gradient in the BLT in the offshore direction (Figure 2a) and no significant seasonal variability (Figures 2c and 2d). The offshore BLT gradient is due to the Atlantic water boundary current transporting warm and saline water from the North Atlantic downstream along the Eurasian continental margins [*Dmitrenko et al.*, 2010]. In the following we focus on the coastal zone and inner shelf, where the seasonal BLT amplitude is maximal and the summer BLT is well above the freezing temperature (Figure 2; see also *Dmitrenko et al.* [2010] for details). In contrast to summer, winter exhibits weak interannual changes (less than ±0.2°C; compare Figures 2c and 2d), with the midshelf and inner-shelf BLTs near the freezing point (not shown). Consequently, we will discuss more specifically the summer BLT tendency in which permafrost-related changes can potentially be important and permafrost can be expected to

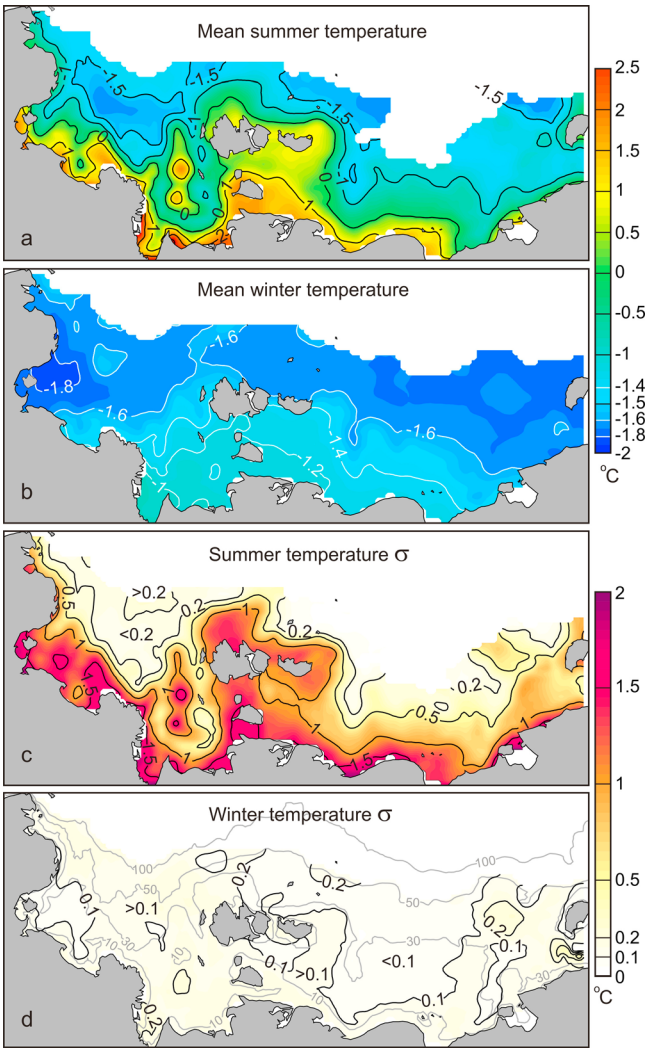

Figure 2. The long-term mean (1920–2009) bottom layer (5 m thick) temperature (°C) for (a) summer and (b) winter with (c, d) their standard deviations σ. Gray numbered lines in 2d show the 10, 30, 50, and 100 m depth contours.

be coldest, deepest, and oldest based on the reconstruction of the Holocene transgression at the North Siberian margin [e.g., *Bauch et al.*, 2001].

[19] The 1920–2009 time series of annual summer mean BLTs and BLSs calculated for the inner shelf and coastal zone of the Laptev and East Siberian seas are shown in Figures 3 and 4, respectively. A quasi-decadal BLT oscillation of approximately ±0.5°C to ±1°C is present, with periods of both bottom layer warming and cooling (Figures 3c and 4c). Both seas exhibit a local bottom temperature minimum around 1962–1964 and 1982–1985, and a local maximum in the late 1950s and 1970s (Figures 3c and 4c). After the mid-1980s, this quasi-decadal periodicity in the coastal BLT is superimposed with a large warming for both the Laptev and East Siberian seas. For the Laptev Sea coastal zone, from 1984 to 2009, the BLT increased by 2.1°C, corresponding to a yearly increase of 0.09°C (Figure 3c). In 2007, the Laptev Sea coastal BLT was at its maximum (~5.9°C) for the entire period of field observations (Figure 3c). While the data coverage over the East Siberian Sea shelf is more sparse in space and not completely continuous in time (Figures 1b and 1c), a similar BLT warming tendency over the coastal zone has been observed since 1984 (Figure 4c). For the coastal zone of both the Laptev and East Siberian seas, the warming trend from the mid-1980s is statistically significant at the 95% confidence level.

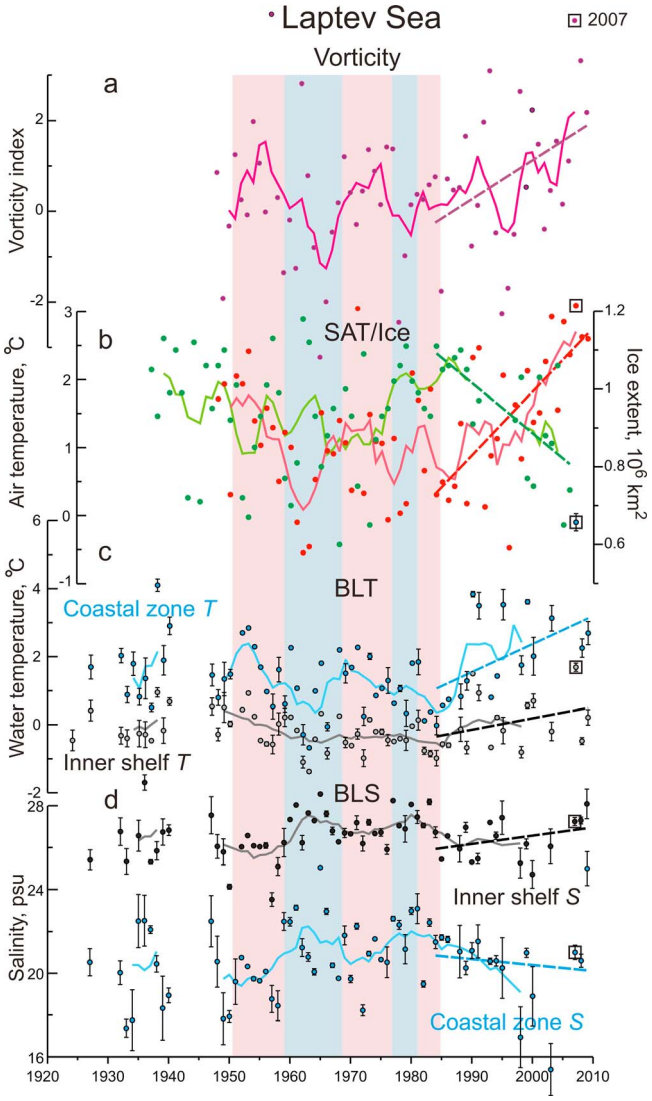

Figure 3. Summer (June–September) mean (a) atmospheric vorticity index (in violet) over the adjacent Arctic Ocean and (b) surface air temperature in red (SAT, °C) and sea ice extent in green (10^6 km^2) over the Laptev Sea. (c, d) Summer bottom layer temperature (BLT, °C) and salinity (BLS, psu) averaged over the Laptev Sea coastal zone (blue dots) and inner shelf (gray and black dots). The error bars show the statistical errors in the annual mean that are due to limited data coverage (for more details see *Dmitrenko et al.* [2008]). Red, green, blue, and gray solid lines show the 5 yr running mean. Bold dashed lines show the 1984–2009 linear trends. For 1951–1984, pink and blue shading highlight positive and negative vorticity anomalies, respectively. The 2007 extreme summer is marked as a black rectangle in each panel.

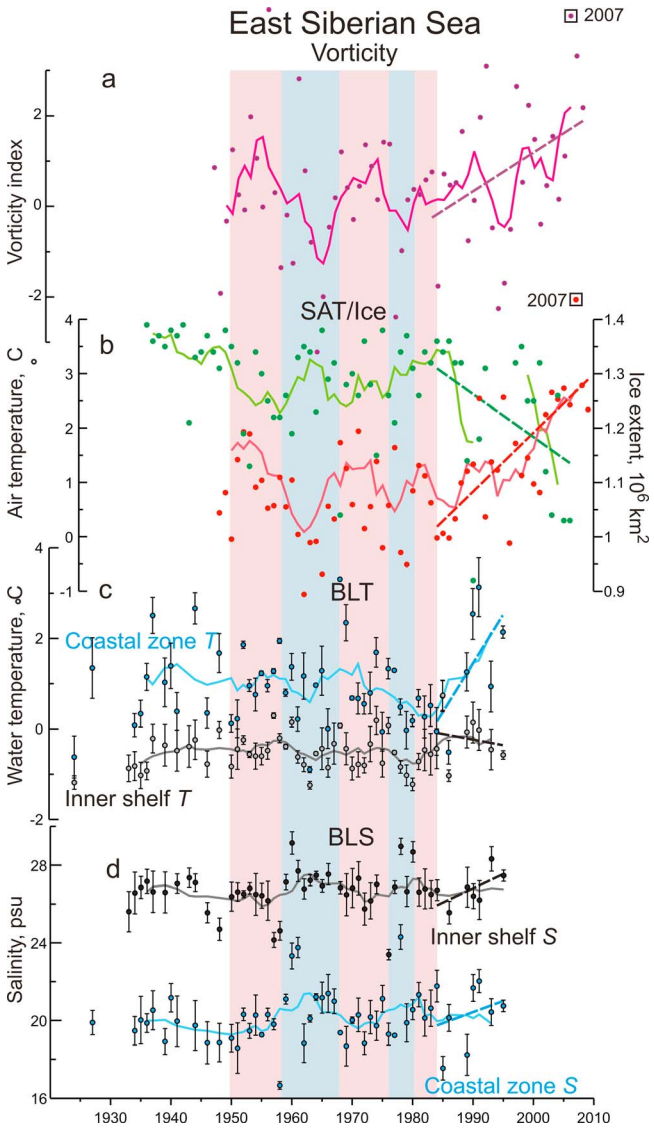

Figure 4. Summer (June–September) mean (a) atmospheric vorticity index (in violet) over the adjacent Arctic Ocean and (b) surface air temperature in red (SAT, °C) and sea ice extent in green (10^6 km^2) over the East Siberian Sea. (c, d) Summer BLT (°C) and BLS (psu) averaged over the East Siberian Sea coastal zone (blue dots) and inner shelf (gray and black dots). Designations are similar to those in Figure 3.

Over the Laptev Sea inner shelf, the warming tendency in the BLT is less pronounced, with the BLT rising by 0.8°C from 1984 to 2009 (Figure 3c). This temperature rise is not statistically significant. In contrast to the Laptev Sea, the East Siberian Sea inner shelf experiences a statistically insignificant cooling of 0.25°C from 1984 to 1995 (Figure 4c).

[20] The 5 year running mean SAT for the Laptev and East Siberian seas is highly correlated with the 5 year running mean atmospheric vorticity (0.59 and 0.64, respectively). These correlations (and others presented later) are statistically significant at the 95% confidence level (Table 2). The summer sea-ice extent, however, shows no correlation with atmospheric vorticity. In contrast, it significantly correlates with summer SATs (−0.50 and −0.79 for the Laptev and East Siberian seas, respectively). As a result of the positive trend in vorticity and SAT over 1984–2009, we observe an enhanced thermodynamic ice melt, a lengthening of the open-water season, as well as more solar heating of the upper water layer. For the vertically mixed water column of the Laptev Sea coastal zone, this results in a BLT highly correlated with SAT (0.69). Despite the strong vertical salinity stratification, this high correlation extends northward over the Laptev Sea inner shelf (0.66). For the East Siberian Sea coastal zone, this correlation is 0.68. For the East Siberian Sea inner shelf, however, the correlation (r = 0.40) is below the 95% level of statistical significance (Table 2). The enhanced sea-ice thermodynamic melting during positive vorticity phases is consistent with bottom layer freshening (Figures 3a, 3d, 4a, and 4d). In fact, the temperature and salinity time series are negatively correlated at −0.64 and −0.61 for the Laptev Sea coastal zone and inner shelf, respectively. The East Siberian Sea inner shelf exhibits similar patterns, with BLTs and BLSs negatively correlated at −0.54. In contrast, for the East Siberian Sea coastal zone, this correlation is not present. Over the Laptev and East Siberian Sea inner shelves, BLSs negatively correlate with atmospheric vorticity (−0.60 and −0.59, respectively; Table 2). A similar, but not statistically significant, correlation between the BLS and vorticity also exists for the Laptev and East Siberian seas coastal zone (−0.43 and −0.37, respectively; Table 2).

[21] For the coastal zone and inner-shelf bottom layer, no thermohaline signature can be clearly attributed to the river discharge interannual variability. This is the case even in 2007, when the Siberian River discharge was maximal over the entire observational record [*Rawlins et al.*, 2009], and the Laptev Sea BLSs were slightly above the climatic mean (Figure 3d).

3.2. Subsea Permafrost Dynamics: Numerical Modeling

[22] Thawing at the upper boundary of subsea permafrost in response to the BLT warming trend during summer (see Figure 5) results in a deepening of the upper boundary of frozen sediments. Our simulation shows that after 25 years of summer BLT warming (as observed from 1985 to 2009), the upper boundary of permafrost deepens by ~1 m (Figure 5). The control run with constant summer temperature and salinity from 1985 onward reveals no deepening of the upper boundary of frozen sediments. The sensitivity

Table 2. Correlation of Potential Atmospheric and Sea-Ice Predictors with BLT and BLS Over the Laptev and East Siberian Sea Subregions 1 and 5 (Coastal Zone) and 2 and 6 (Inner Shelf)[a]

	BLT				BLS			
	Laptev Sea Subregions		East Siberian Sea Subregions		Laptev Sea Subregions		East Siberian Sea Subregions	
	1	2	5	6	1	2	5	6
Vorticity	0.47	0.40	0.41	0.29	−0.43	**−0.60**	−0.37	**−0.59**
SAT	**0.69**	**0.66**	**0.68**	0.40	X	X	−0.29	X
SIE	**−0.51**	**−0.51**	**−0.54**	**−0.50**	X	X	X	X

[a]Statistically significant correlations (at 95% confidence level) are indicated by bold numbers. Crosses indicate no correlation.

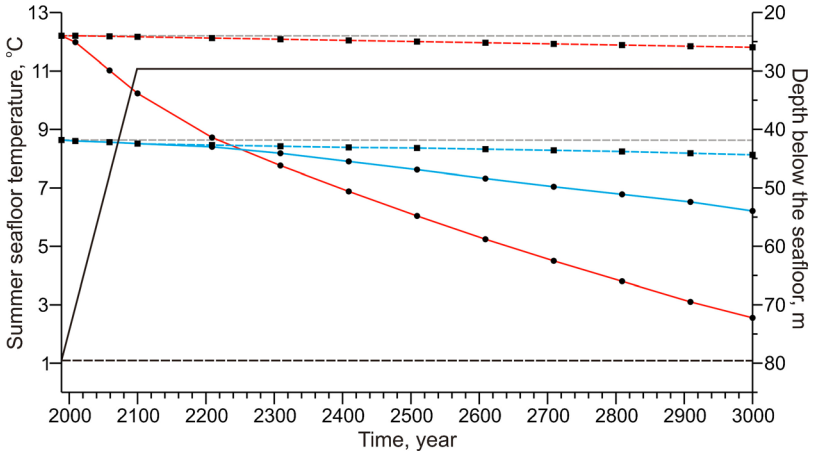

Figure 5. Simulated permafrost downward degradation after 1985. Red and blue solid lines show the upper boundary of frozen sediments and interface between fresh and salt-contaminated sediments, respectively, in response to the warming trend since 1985. Red and blue dashed lines show the same, but without the temperature trend. The solid black line shows the summer seafloor temperature used as boundary condition for the case with temperature trend. Constant-temperature boundary conditions set at the summer long-term (1920–1984) mean BLT (1.1°C, dashed black line) are used for the case with no temperature trend. The seasonal cycle is not shown.

experiment for the time period 2009 to 2100 (with a linear summer BLT trend) and 2100 to 3000 (with a constant summer BLT of 11.5°C) shows a permafrost table deepening of ~5 m after 50 years, ~9 m after 100 years, and ~48 m after 1000 years relative to its modern provisional state in 2009 (Figure 5). Over the same time periods, the control runs without BLT trends show a deepening of the permafrost table by 0.1 m, 0.2 m, and 2 m, respectively. Overall, the modeling results show enhanced rates in downward subsea permafrost degradation (~0.10 m/yr) from 2010 to 2100, while, for 1985–2009 and 2100–3000, it is significantly slower (~0.04 m/yr). Up to 96% of this degradation is associated with the imposed warming trend. The rest is due to the response of the permafrost to the submergence of the continental shelf ~8000 years B.P.. After year ~2240, the thawing front extends deeper than the interface between fresh and salt-contaminated sediments (heat diffusion is faster than salt diffusion), and sediments below the thawing front remain frozen at temperatures below their freezing point temperature of 0°C (Figure 6).

[23] Figure 6 shows the temporal evolution of vertical temperature profiles across the upper 250 m below the seafloor. For 1985, the simulated temperature profile (dark blue line) shows an ~1°C difference from those modeled by *Delisle* [2000] (black line), in part because of the effect of salt diffusion, which is taken into account in the present simulation, but more important because of the difference in the upper boundary condition for temperatures taken by *Delisle* [2000] (constant −1.5°C) compared with the one used in this study (seasonal cycle included). In fact, this offset is a measure of the modeling uncertainty to the temperature boundary condition, an unknown for the time period before the era of instrumental observations. The upper 4 m layer with the highest temperature gradients represents the active layer with the most significant seasonal changes in temperature [e.g., *Osterkamp et al.*, 1989].

[24] In general, the simulated physical properties of subsea sediments for 1985 (Figure 6) are consistent with those measured in 2005 from a seafloor drilling program in the Laptev Sea coastal zone at ~7 m water depth [*Rachold et al.*, 2007]. The upper layer of sediments down to the depth of 30 m below the seafloor has been found unfrozen at ~−1°C, with pore water salinity ranging from 4 psu above the permafrost layer to 24 psu near the seafloor. The underlying frozen sediment temperature observations range from −1°C to −1.6°C with a salinity of ~1.5 psu [*Rachold et al.*, 2007]. Similar to the results of direct measurements for 2005, the simulated temperature of sediments down to 25 m is below 0°C (dark blue line in Figure 6). Note that the sediments can still remain unfrozen because of the salt contamination. However, the model results clearly show a warming from 1985 onward, down to ~30–70 m (Figure 6). This is in contrast with results from *Rachold et al.* [2007] and *Junker et al.* [2008] that show almost-constant temperature profiles. This indicates that summer BLT warming, observed in the region since 1985, was not yet sufficient to trigger noticeable changes in subsea sediments of the Laptev Sea coastal zone.

4. Discussion: Siberian Shelf Environment and Potential for Subsea Permafrost Instability in the Siberian Arctic

[25] Results from a multiple correlation between BLTs and various atmospheric and sea-ice indices (Table 2) show that, during summer, the inner shelf and coastal bottom layer are mainly controlled by atmospheric vorticity on quasi-decadal timescales. The BLT generally cools when the vorticity index is negative (anticyclonic) and warms when the vorticity index is positive (cyclonic) because of cold-warm air advection during negative-positive vorticity phases (Figures 3a, 3c, 4a, and 4c and Table 2). Our results also

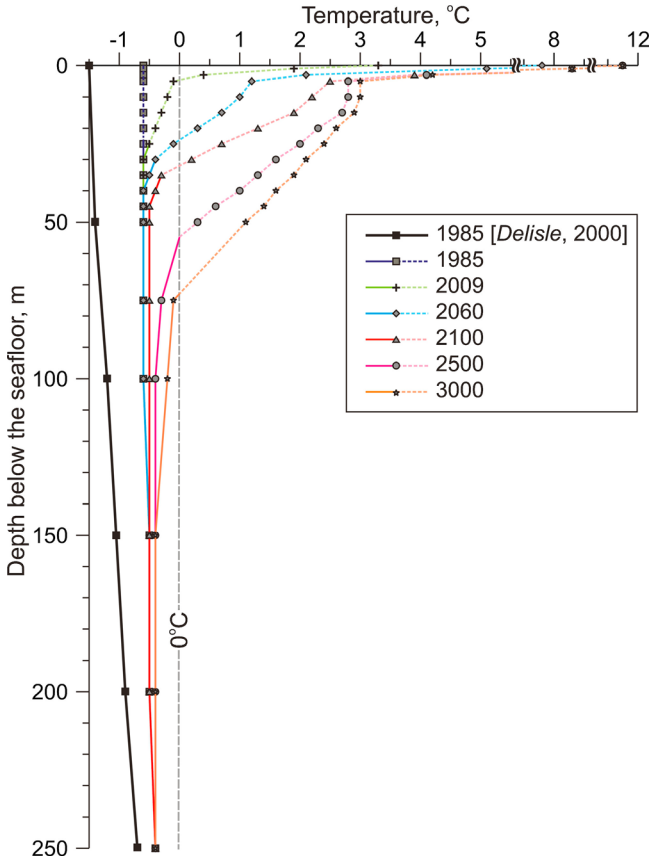

Figure 6. Subsea permafrost degradation after 1985. Shown is the summer mean temperature field as a function of depth, for different times, starting from 1985 until 3000. Solid and dashed lines show temperature profiles across frozen and thawed sediments, respectively. Boundary conditions are described in section 2.2 and Figure 5. For calculating temperature profiles for 1985 (dark blue line), the long-term (1920–1984) seasonal mean summer and winter temperatures are taken from the Laptev Sea coastal zone at 1.1°C and −1.4°C, respectively. The bold black line shows vertical temperature profiles for 1985 simulated by *Delisle* [2000] for a constant mean annual seafloor temperature of −1.5°C.

clearly show evidence for increased SAT and enhanced atmospheric cyclonicity over the eastern Siberian shelf since the mid-1980s (Figures 3a, 3b, 4a, and 4b). This is consistent with enhanced summer cyclonicity over the Eurasian Basin from 1979 to 2008 [*Simmonds et al.*, 2008; *Simmonds and Keay*, 2009]. The reason for the sea-ice decline is in part due to a lengthening of the open-water season and consequently more solar heating of the upper water layer [*Steele et al.*, 2008].

[26] Using satellite passive microwave data from 1979 to 2007, *Markus et al.* [2009] reported a statistically significant (at the 99% confidence level) positive tendency in the freezeup onset by 7 days/decade in the Laptev and East Siberian seas. This is the largest trend recorded over the entire Arctic Ocean area. Over the same time period, a negative trend in melt onset (i.e., toward an earlier melt) of 3 days/decade (statistically significant at the 95% confidence level) was observed [*Markus et al.*, 2009]. Overall, the Laptev and East Siberian seas exhibit a positive trend in melt season length of ~10.5 days/decade. This is among the top four regions of the Arctic Ocean with the greatest trends in melt season length (the other three regions are Hudson Bay, the East Greenland Sea, and the Chukchi/Beaufort seas). Over the eastern Siberian shelf, the melt season has lengthened by almost 30 days since 1979 [*Markus et al.*, 2009].

[27] Over the coastal zone, where the water column is well mixed, the surface heating directly impacts the bottom layer temperature. For the vertically stratified water of the inner shelf, the surface heating penetrates down to the seafloor through wind-forced mixing associated with storm events. The enhanced summer cyclonicity over the Eurasian Basin also results in an eastward diversion in the river water pathways along the eastern Siberian coast and the formation of coastal currents [*Dmitrenko et al.*, 2008]. Over the Laptev and East Siberian seas inner shelves and coastal zone, the negative correlation between the BLS and atmospheric vorticity (Table 2) points to the role of alongshore eastward wind-driven fresh water transport from the Laptev Sea to the East Siberian Sea during the positive vorticity phase [*Dmitrenko et al.*, 2008]. This supports our general assessment that the sea-ice melting due to positive SAT anomalies together with eastward flowing riverine water results in bottom layer freshening when the cyclonicity of the atmosphere is positive. In general, this also implies the role of vertical mixing in transporting fresh and warm water anomalies downward to the seafloor. In contrast to the cyclonic regime, anticyclonic atmospheric circulation results in the influx of more saline waters from the Chukchi Sea into the East Siberian Sea [*Dmitrenko et al.*, 2005; *Semiletov et al.*, 2005] and riverine water migration from the eastern Siberian shelf to the Arctic Ocean through the northeastern Laptev Sea [*Dmitrenko et al.*, 2008]. This implies one important consequence for the Siberian shelf environment and bottom layer hydrography. Weaker density stratification over the inner shelf favors enhanced wind-driven vertical mixing and bottom layer ventilation in summer and fall that leads to additional warming of the bottom layer. Our results presented in section 3.1 are broadly consistent with this assessment. In summary, our hydrographic data show a dramatic warming of the bottom water layer over the eastern Siberian shelf coastal zone since the mid-1980s by 2.1°C, which is attributed to changes in the Arctic atmosphere.

[28] There are several models that explore thermal adjustment and dynamics of the submerged frozen ground to changes in seafloor temperatures, along with other factors, including enhanced geothermal heat fluxes in areas underlain by fault zone [*Romanovskii and Hubberten*, 2001], thermal effects of riverine water [*Delisle*, 2000], and thermokarst [*Nicolsky and Shakhova*, 2010]. All these studies consider that a thermal adjustment of frozen ground to a temperature increase is associated with inundation that occurred ~8000 years B.P. In addition, in all these studies, a constant annual mean seafloor temperature is assumed following the inundation. Modeling shows that, at present, away from the geomorphologic and geological patterns like thermokarst depressions, river paleovalleys, fault zones etc., the subsea permafrost is still adjusting to the 12°C warming, with a reduced temperature gradient at the base of the permafrost layer, leading to slow upward degradation that is due to geothermal heat flux [*Delisle*, 2000; *Romanovskii*

and Hubberten, 2001]. Control simulations made without marine salt diffusion into the permafrost are consistent with these results [*Nicolsky and Shakhova*, 2010]. Model runs including salt diffusion revealed a significant layer of thawed ground material down to a depth of ~100 m overlaying the frozen sediments [*Nicolsky and Shakhova*, 2010]. In general, our hindcast simulation for 1985 (Figure 6) is consistent with this study. However, our modeling shows thinner layers of unfrozen sediments (~25 m), which is in agreement with direct observations by *Rachold et al.* [2007].

[29] In contrast to the cited modeling studies, the primary purpose of our research is to evaluate the potential effect of recent climatic warming on the subsea permafrost instability. In our forecast simulation we use extreme and schematic climate scenarios, rather than any of the Intergovernmental Panel on Climate Change (IPCC) projections. For example, for the Laptev Sea coastal zone from 1985 to 2009, we observe a 2.1°C increase in the summer BLT in response to a 2.5°C increase in the summer SAT (Figures 3b and 3c). For the time period from 2010 to 2100, the summer BLT increases linearly from ~3°C to 11.5°C (i.e., an 8.5°C increase; see Figure 5). In contrast, for the Laptev Sea coastal zone, the IPCC projects a summer sea surface temperature (SST) increase of only 3°C–4°C [e.g., *Teng et al.*, 2006]. For the chosen climate scenario, our modeling clearly shows a warming of sediments from 1985 onward, down to ~30–70 m (Figure 6), with a thawing front propagating downward from 5 m after 50 years, 9 m after 100 years, and 48 m after 1000 years of experiencing the BLT trend (Figure 5). Is this important for the liberation of methane or not?

[30] We have been motivated by the potential of subsea permafrost thawing and GHSZ instability to produce rapid releases of methane in response to recent climate changes. Based on numerical simulations [*Delisle*, 2000; *Romanovskii et al.*, 2005], the upper boundary of the GHSZ over the Siberian shelf coastal regions lies within the permafrost at a depth ~200 m below the seafloor (note that seismic profiling in the Laptev Sea midshelf reveals a signature of the CH_4-enriched sediments already ~10–15 m below the seafloor [*Rekant et al.*, 2009]). However, it remains unclear whether some CH_4 hydrates can also be stored within the permafrost layer and, if so, how big this reservoir is [*O'Connor et al.*, 2010].

[31] The simulated impact of the summer BLT warming on projected degradation of subsea permafrost (at most ~1 m) from 1985 to 2009 is not significant for enhancing CH_4 emission from the thawed sediments. Recent and projected constant warming trends over the next 50 and 100 years will affect only the upper tens of meters of the subsea permafrost (Figures 5 and 6). Indeed, the response time of permafrost thawing (centuries) to the seafloor warming is long compared with the timescale of the recent instrumental record of CH_4 emissions (decades), and therefore the enhanced rate of CH_4 emissions in response to recent climate warming cannot yet be detected.

5. Summary and Conclusions

[32] Summer hydrographic data (1920–2009) show a dramatic warming of the bottom water layer over the eastern Siberian shelf coastal zone (<10 m depth) since the mid-1980s, by 2.1°C. We attribute this warming to changes in the Arctic atmosphere. The enhanced summer cyclonicity results in warmer air temperature and a reduction in ice extent, mainly through thermodynamic melting. This leads to a lengthening of the summer open-water season and to more solar heating of the water column.

[33] The permafrost modeling shows that a significant change in the permafrost depth lags behind the imposed changes in surface temperature. Thus, a significant degradation of subsea permafrost is expected to be detectable only at the beginning of the next millennium. Until that time (the year 3000), the simulated permafrost table shows a deepening down to ~70 m below the seafloor (Figure 5). This depth of the frozen permafrost is still less than that of the GHSZ, but only within errors of the simulated depth of the GHSZ upper boundary. Taking into account the uncertainties in the simulated results and lack of direct observations, this deepening is considered to be important for the stability of the subsea permafrost and the GHSZ.

[34] In summary, our results do not support the hypothesis that the recent CH_4 supersaturation, reported by *Shakhova et al.* [2010], was triggered by recent Arctic climate changes. Instead, it is more likely the result of the continuous degradation of subsea permafrost associated with the warming initiated by permafrost submergence ~8000 years B.P.. Overall, while our data provide evidence of drastic bottom layer heating over the coastal zone during summer, the increase in temperature could not produce an immediate response in thawing the subsea Arctic permafrost causing the increase in methane emission. In this context, we share a viewpoint of *Petrenko et al.* [2010] that "a newly discovered CH_4 source is not necessarily a changing source, much less a source that is changing in response to Arctic warming." Marine hydrates are destabilized on timescales of millennia because of the large inertia associated with oceanic circulation and heat propagation in sediments [*O'Connor et al.*, 2010]. Continuing climate change, however, may significantly increase summer seafloor bottom temperatures over the coastal zone, which may have an important impact on the stability of offshore submarine permafrost already in the next millennium.

[35] **Acknowledgments.** We acknowledge the financial support through the BMBF project "System Laptev Sea." O.A.A. and S.A.L. acknowledge the support by the Russian Foundation for Basic Research through grant 11-05-12011. We greatly appreciate Paul Overduin (AWI-Potsdam, Germany) and Tina Treude (IFM-GEOMAR, Germany) for their helpful comments and discussions. Three anonymous reviewers provided helpful comments and criticism.

References

Anisimov, O. A., S. A. Lavrov, and S. A. Reneva (2005), Modeling the emission of greenhouse gases from the Arctic wetlands under the conditions of the global warming, in *Climatic and Environmental Changes* [in Russian], edited by G. V. Menzhulin, pp. 21–39, Hydrometeoizdat, St. Petersburg, Russia.

Bauch, H. A., T. Mueller-Lupp, E. Taldenkova, R. F. Spielhagen, H. Kassens, P. M. Grootes, J. Thiede, J. Heinemeier and V. V. Petryashov (2001), Chronology of the Holocene transgression at the North Siberian margin, *Global Planet. Change*, *31*, 125–139, doi:10.1016/S0921-8181(01)00116-3.

Comiso, J. C., C. L. Parkinson, R. Gersten, and L. Stock (2008), Accelerated decline in the Arctic sea ice cover, *Geophys. Res. Lett.*, *35*, L01703, doi:10.1029/2007GL031972.

Delisle, G. (2000), Temporal variability of sub-sea permafrost and gas hydrate occurrences as function of climate change in the Laptev Sea, Siberia, *Polarforschung*, *68*, 221–225.

Dmitrenko, I., S. Kirillov, H. Eicken, and N. Markova (2005), Wind-driven summer surface hydrography of the eastern Siberian shelf, *Geophys. Res. Lett.*, *32*, L14613, doi:10.1029/2005GL023022.

Dmitrenko, I. A., S. A. Kirillov, and L. B. Tremblay (2008), The long-term and interannual variability of summer fresh water storage over the eastern Siberian shelf: Implication for climatic change, *J. Geophys. Res.*, *113*, C03007, doi:10.1029/2007JC004304.

Dmitrenko, I. A., S. A. Kirillov, L. B. Tremblay, D. Bauch, and S. Willmes (2009), Sea-ice production over the Laptev Sea shelf inferred from historical summer-to-winter hydrographic observations of 1960s–1990s, *Geophys. Res. Lett.*, *36*, L13605, doi:10.1029/2009GL038775.

Dmitrenko, I. A., S. A. Kirillov, L. B. Tremblay, D. Bauch, J. A. Hölemann, T. Krumpen, H. Kassens, C. Wegner, G. Heinemann, and D. Schröder (2010), Impact of the Arctic Ocean Atlantic water layer on Siberian shelf hydrography, *J. Geophys. Res.*, *115*, C08010, doi:10.1029/2009JC006020.

Fleming, K., P. Johnston, D. Zwartz, Y. Yokoyama, K. Lambeck, and J. Chappell (1998), Refining the eustatic sea-level curve since the last glacial maximum using far- and intermediate-field sites, *Earth Planet. Sci. Lett.*, *163*, 327–342, doi:10.1016/S0012-821X(98)00198-8.

Junker, R., M. N. Grigoriev, and N. Kaul (2008), Non-contact infrared temperature measurements in dry permafrost boreholes, *J. Geophys. Res.*, *113*, B04102, doi:10.1029/2007JB004946.

Kalnay, E. M., et al. (1996), The NCEP/NCAR 40-year reanalysis project, *Bull. Am. Meteorol. Soc.*, *77*, 437–471, doi:10.1175/1520-0477(1996)077<0437:TNYRP>2.0.CO;2.

Kwok, R., and D. A. Rothrock (2009), Decline in Arctic sea ice thickness from submarine and ICESat records: 1958–2008, *Geophys. Res. Lett.*, *36*, L15501, doi:10.1029/2009GL039035.

Kwok, R., G. F. Cunningham, M. Wensnahan, I. Rigor, H. J. Zwally, and D. Yi (2009), Thinning and volume loss of the Arctic Ocean sea ice cover: 2003–2008, *J. Geophys. Res.*, *114*, C07005, doi:10.1029/2009JC005312.

Mahoney, A. (2008), *Sea Ice Edge Location and Extent in the Russian Arctic, 1933–2006, digital media*, Nat. Snow Ice Data Cent., Boulder, Colo.

Mahoney, A. R., R. G. Barry, V. Smolyanitsky, and F. Fetterer (2008), Observed sea ice extent in the Russian Arctic, 1933–2006, *J. Geophys. Res.*, *113*, C11005, doi:10.1029/2008JC004830.

Markus, T., J. C. Stroeve, and J. Miller (2009), Recent changes in Arctic sea ice melt onset, freezeup, and melt season length, *J. Geophys. Res.*, *114*, C12024, doi:10.1029/2009JC005436.

Nicolsky, D., and N. Shakhova (2010), Modeling sub-sea permafrost in the East Siberian Arctic Shelf: The Dmitry Laptev Strait, *Environ. Res. Lett.*, *5*, 015006, doi:10.1088/1748-9326/5/1/015006.

O'Connor, F. M., et al. (2010), Possible role of wetlands, permafrost, and methane hydrates in the methane cycle under future climate change: A review, *Rev. Geophys.*, *48*, RG4005, doi:10.1029/2010RG000326.

Osterkamp, T., G. Baker, W. Harrison, and T. Matava (1989), Characteristics of the active layer and shallow subsea permafrost, *J. Geophys. Res.*, *94*(C11), 16,227–16,236, doi:10.1029/JC094iC11p16227.

Peterson, B. J., J. McClelland, R. Curry, R. M. Holmes, J. E. Walsh, and K. Aagaard (2006), Trajectory shifts in the Arctic and subarctic freshwater cycle, *Science*, *313*, 1061–1066, doi:10.1126/science.1122593.

Petrenko, V. V., D. M. Etheridge, R. F. Weiss, E. J. Brook, H. Schaefer, J. P. Severinghaus, A. M. Smith, D. Lowe, Q. Hua, and K. Riedel (2010), Methane from the East Siberian Arctic Shelf, *Science*, *329*, 1146–1147, doi:10.1126/science.329.5996.1146-b.

Polyakov, I. V., V. A. Alexeev, G. I. Belchansky, I. A. Dmitrenko, V. V. Ivanov, S. A. Kirillov, A. A. Korablev, M. Steele, L. A. Timokhov, and I. Yashayaev (2008), Arctic Ocean freshwater changes over the past 100 years and their causes, *J. Clim.*, *21*, 364–384, doi:10.1175/2007JCLI1748.1.

Rachold, V., R. Junker, F. Merker, P. Overduin, H.-W. Hubberten, M. N. Grigoriev, D. Y. Bolshiyanov, V. V. Kunitsky, and W. Schneider (2007), Nearshore Arctic Subsea Permafrost in Transition, *Eos Trans. AGU*, *88*(13), doi:10.1029/2007EO130001.

Rawlins, M. A., M. C. Serreze, R. Schroeder, X. Zhang, and K. C. McDonald (2009), Diagnosis of the record discharge of Arctic-draining Eurasian rivers in 2007, *Environ. Res. Lett.*, *4*, 045011, doi:10.1088/1748-9326/4/4/045011.

Reagan, M. T., and G. J. Moridis (2007), Oceanic gas hydrate instability and dissociation under climate change scenarios, *Geophys. Res. Lett.*, *34*, L22709, doi:10.1029/2007GL031671.

Rekant, P. V., V. E. Tumskoi, E. A. Gusev, T. Schwenk, F. Spiess, G. A. Chercashev, and H. Kassens (2009), Distribution and peculiarities of bedding of the subsea permafrost near Semenovskoe and Vasilievskoe shoals revealed by high-resolution seismic profiling, in *System of the Laptev Sea and the Adjacent Arctic Seas [in Russian]*, edited by H. Kassens, pp. 332–348, Moscow Univ. Press, Moscow.

Romanovskii, N. N., and H.-W. Hubberten (2001), Results of permafrost modeling of the lowlands and shelf of the Laptev Sea region, Russia, *Permafrost Periglacial Processes*, *12*(2), 191–202, doi:10.1002/ppp.387.

Romanovskii, N. N., H.-W. Hubberten, A. V. Gavrilov, V. E. Tumskoy, and A. L. Kholodov (2004), Permafrost of the east Siberian Arctic shelf and coastal lowlands, *Quat. Sci. Rev.*, *23*, 1359–1369, doi:10.1016/j.quascirev.2003.12.014.

Romanovskii, N. N., H.-W. Hubberten, A. V. Gavrilov, A. A. Eliseeva, and G. S. Tipenko (2005), Offshore permafrost and gas hydrate stability zone on the shelf of East Siberian Seas, *Geo Mar. Lett.*, *25*, 167–182, doi:10.1007/s00367-004-0198-6.

Semiletov, I., O. Dudarev, V. Luchin, A. Charkin, K.-H. Shin, and N. Tanaka (2005), The East Siberian Sea as a transition zone between Pacific-derived waters and Arctic shelf waters, *Geophys. Res. Lett.*, *32*, L10614, doi:10.1029/2005GL022490.

Shakhova, N., and I. Semiletov (2009), *Arctic Climate Feedbacks: Global Implications*, edited by M. Sommerkorn and S. J. Hassol, pp. 81–92, WWF Int. Arctic Programme, Oslo.

Shakhova, N. E., V. I. Sergienko, and I. P. Semiletov (2009), The contribution of the East Siberian shelf to the modern methane cycle, *Herald Russ. Acad. Sci.*, *79*, 237–246, doi:10.1134/S101933160903006X.

Shakhova, N., I. Semiletov, A. Salyuk, V. Yusupov, D. Kosmach, and Ö. Gustafsson (2010), Extensive methane venting to the atmosphere from sediments of the East Siberian Arctic shelf, *Science*, *327*, 1246–1250, doi:10.1126/science.1182221.

Simmonds, I., and K. Keay (2009), Extraordinary September Arctic sea ice reductions and their relationships with storm behavior over 1979–2008, *Geophys. Res. Lett.*, *36*, L19715, doi:10.1029/2009GL039810.

Simmonds, I., C. Burke, and K. Keay (2008), Arctic climate change as manifest in cyclone behaviour, *J. Clim.*, *21*, 5777–5796, doi:10.1175/2008JCLI2366.1.

Steele, M., W. Ermold, and J. Zhang (2008), Arctic Ocean surface warming trends over the past 100 years, *Geophys. Res. Lett.*, *35*, L02614, doi:10.1029/2007GL031651.

Stroeve, J., S. Drobot, S. Gearheard, T. Scambos, M. Serreze, J. Maslanik, W. Meier, and M. Holland (2008), Arctic Sea Ice Extent Plummets in 2007, *Eos Trans. AGU*, *89*(2), 13, doi:10.1029/2008EO020001.

Teng, H., W. M. Washington, G. A. Meehl, L. E. Buja, and G. W. Strand (2006), Twenty-first century Arctic climate change in the CCSM3 IPCC scenario simulations, *Clim. Dyn.*, *26*, 601–616, doi:10.1007/s00382-005-0099-z.

Walsh, J. E., W. L. Chapman, and T. Shy (1996), Recent decrease of sea level pressure in the central Arctic, *J. Clim.*, *9*, 480–486, doi:10.1175/1520-0442(1996)009<0480:RDOSLP>2.0.CO;2.

Westbrook, G. K., et al. (2009), Escape of methane gas from the seabed along the West Spitsbergen continental margin, *Geophys. Res. Lett.*, *36*, L15608, doi:10.1029/2009GL039191.

O. A. Anisimov and S. A. Lavrov, Department of Climate Change Research, State Hydrological Institute, 23 2nd Line VO, St. Petersburg 199053, Russia.

I. A. Dmitrenko and H. Kassens, Leibniz Institute of Marine Sciences, University of Kiel, Wischhofstr. 1–3, Kiel D-24148, Germany. (idmitrenko@ifm-geomar.de)

M. N. Grigoriev and S. O. Razumov, Melnikov Permafrost Institute, Siberian Branch of the Russian Academy of Science, 36 Merzlotnaya St., Yakutsk 677010, Russia.

S. A. Kirillov, Arctic and Antarctic Research Institute, 38 Bering St., St. Petersburg 199397, Russia.

L. B. Tremblay, Department of Atmospheric and Oceanic Sciences, McGill University, 805 Sherbrooke St. W., Montreal, QC H3A 2K6, Canada.